Remineralising effects of fluoride varnishes containing calcium phosphate on artificial root caries lesions with adjunctive application of proanthocyanidin

Cai, Jing; Burrow, Michael F.; Manton, David J.; Hardiman, Rita; Palamara, Joseph E.A.

Published in:
DENTAL MATERIALS

DOI:
10.1016/j.dental.2020.10.021

Publication date:
2021

DENTAL MATERIALS 37 (2021) 143–157

Available online at www.sciencedirect.com

ScienceDirect

journal homepage: www.intl.elsevierhealth.com/journals/dema

Remineralising effects of fluoride varnishes containing calcium phosphate on artificial root caries lesions with adjunctive application of proanthocyanidin

Jing Cai[a], *Michael F. Burrow*[a,b], *David J. Manton*[a,c], *Rita Hardiman*[a], *Joseph E.A. Palamara*[a,*]

[a] *Melbourne Dental School, The University of Melbourne, 720 Swanston Street, Carlton, VIC 3053, Australia*
[b] *Faculty of Dentistry, the University of Hong Kong, Prince Philip Dental Hospital, Sai Ying Pun, Hong Kong SAR, China*
[c] *Centrum voor Tandheelkunde en Mondzorgkunde, UMCG, University of Groningen, The Netherlands*

ARTICLE INFO

Keywords:
proanthocyanidin
CPP-ACP
TCP
fluoride varnish
dentinal organic matrix
root caries

ABSTRACT

Objectives. To evaluate the remineralising effects of fluoride (F) varnishes containing bioavailable calcium-phosphate compound (Ca-P) based remineralisation systems and 5000 ppm F toothpaste (FTP) on root caries lesions (RCLs) and the potential effects of proanthocyanidin (PA) for the treatments of RCLs when used as an adjunct to F regimens.

Methods. Demineralised root dentine and a pH-cycling model were used to mimic RCLs and the oral environment. Remineralising effects of MI Varnish™ (MIV) containing casein phosphopeptide–amorphous calcium phosphate (CPP-ACP) and Clinpro™ White Varnish (CPWV) containing tri-calcium phosphate (TCP) along with FTP and PA were evaluated regarding the birefringence, elemental composition, mechanical properties and mineral density of remineralised dentine with Duraphat™ as a comparison.

Results. MIV, CPWV and Duraphat™ promoted the incorporation of F into RCLs and increased mineral density but did not change microhardness of root dentine significantly. Surface microhardness increased significantly when MIV or CPWV was used with 5000 ppm FTP. Application of PA with F regimens significantly increased subsurface mineral density. When PA was applied with MIV or CPWV along with FTP, the highest ion uptake and relative mineral gain (%ΔZ) was achieved, and significant increase of microhardness was up to 30 μm depth. Generally, MIV was associated with a higher mineral content gain than CPWV.

Significance. Treatment of carious root surfaces remains challenging due to the complex pathological processes and difficulty in restoring the highly organised structure of root dentine. Treatment strategies targeting both remineralisation and preservation of the dentinal organic matrix have the potential to improve the fluoride-mediated remineralisation approaches.

* Corresponding author at: Melbourne Dental School, University of Melbourne, 720 Swanston St, Carlton, VIC, 3053, Australia.
E-mail address: palamara@unimelb.edu.au (J.E.A. Palamara).

https://doi.org/10.1016/j.dental.2020.10.021

1. Introduction

Increasing tooth retention in ageing populations in industrialised countries and the age-related recession of gingival tissues exposing tooth root surfaces to the oral environment have contributed significantly to the increasing prevalence of root caries amongst the elderly [1,2]. Current treatments following caries management philosophies established for enamel caries may not be equally efficacious for root dentine caries because of the different structures and compositions of enamel and dentine and the associated distinct aetiologies and disease progression of coronal and root caries [3].

Dentine is an hierarchically organised nanocrystalline composite structure formed by matrix-mediated mineralisation. The organic framework of dentine consists of parallel self-assembled 300 nm long collagen units composed of collagen fibrils of 67 nm periodicity staggered and overlapped along their long axes and stabilised by covalent inter- and intramicrofibrillar cross-linking [4,5]. The gap spaces between the collagen molecular ends are the primary sites for nucleation and growth of the plate-like impure hydroxyapatite crystals [6]. This structural and stereochemical matching between inorganic and organic materials confers dentine with specific mechanical properties and promotes synergy between matrix and mineral during the caries process [7]. Specifically, in the early stages of caries development, the pH decrease produced by metabolites of acidogenic bacteria tilts the balance of de- and re-mineralisation towards mineral dissolution - especially of the extrafibrillar minerals. Mineral loss affects the packing arrangement of the fibrils and activates the host proteases along with bacterial collagenase action, leading to lysis of dentinal collagen. The loss of collagen periodicity and the shifts of inter-molecular cross-linkages of the molecules of dentinal collagen result in further loss of intrafibrillar minerals, decreasing the mechanical properties of dentine [8,9].

Demineralisation can be reversed in its early stages through incorporation of component ions (calcium, phosphate and fluoride) onto the remnant nano-crystallites [10]. Fluoride (F) is currently considered the gold standard therapeutic agent for early carious lesions. It deposits on tooth surfaces as CaF_2-like materials and substitutes into dental mineral through dissolution/re-precipitation reactions to form an apatitic mineral of increased structural stability - $Ca_5(PO_4)_3(OH)_{1-x}F_x$ [11,12]. Given that root dentine has a higher critical pH and smaller impure hydroxyapatite crystallites than enamel, there is clinically validated consensus that high concentration F toothpastes (FTP) and F varnishes are recommended to maintain the mineral balance in root caries lesions (RCLs) and the efficacy of F treatments could be further enhanced by a combination of F delivery methods [10,13]. In addition, the availability of calcium and phosphate (mainly from saliva and gingival crevicular fluid) is rate limiting for remineralisation. Ageing and medication in elders could affect salivary flow and constituents and decrease the availability of calcium and phosphate for restoring mineral density of RCLs [14]. Therefore, bioavailable calcium-phosphate compound (Ca-P) based remineralisation systems have been incorporated and stabilised into F products to promote remineralisation [11]. Nevertheless, it is still controversial whether the addition of Ca-P has superior effects over F alone, as well as the relative efficacy of different Ca-P based remineralisation systems [15–18]. In particular, there is a lack of published evidence of their effectiveness on RCLs.

Whilst F treatments in combination with calcium and phosphate restore the mineral content of carious lesions, poorly remineralised tissue with majority of minerals occupying extrafibrillar space and decreased strength of collagen fibrils may not recover the overall functionality of dentine [7]. Increasing understanding of the hierarchical structure and biochemistry of dentine has promoted the advent of innovative biomimetic approaches for treatment of dentine carious lesions. Specifically, the presence of dentinal collagen could putatively provide a template and exert spatial constraints to mediate spherulitic crystalline growth of minerals after infiltration of ionic clusters of mineralisation precursors containing Ca-P [19,20]. Therefore, strategies for dentinal collagen biomodification to prevent degradation of the demineralised matrix have been explored to enhance the interaction of minerals within the collagen fibrils [21,22]. Locally applied collagenase inhibitors such as chlorhexidine and Zn^{2+} could inhibit the activity of proteolytic enzymes during dentine demineralisation and reduce dentine matrix degradation, thus limiting lesion progression [23–25]. However, inhibitors might not affect all proteases involved in the degradation process. On the other hand, when affected by collagenase, the cross-links of dentinal organic matrix are partially shifted to precursors whilst the collagen matrix is not structurally and biochemically different from that of sound dentine, therefore, it has the potential to revert to normal collagen fibres [26]. In this regard, induction of cross-linking might have the ability to recover the structure of dentinal collagen [27]. Particularly, chemical cross-linking using agents such as glutaraldehyde and 1-ethyl-3-(3-dimethylaminopropyl)carbodiimide/N-hydroxysuccinimide (EDC/NHS) are the most effective strategies to produce a uniform and high degree of cross-linking in dentine, however, their cytotoxicity may be a limitation for clinical applications [28,29]. Biocompatible natural cross-linkers, mostly polyphenols, have received increasing attention in recent decades. Amongst them, proanthocyanidin (PA), derived from grape seed extracts, holds great potential to cross-link dentinal collagen by covalent and ionic linkages as well as hydrogen bonds and hydrophobic interaction [30]. Previous studies have reported that application of PA increased the mechanical properties of demineralised dentine and enhanced the remineralisation of RCLs by stabilising collagen [28,31]. Adjunctive application of PA with F/Ca/P showed promising results in improving mineral gain and mechanical properties as well as preventing proteolytic biodegradation in dentine [32–34]. Considering the potential beneficial effects of PA, we were motivated to investigate the strategy of application of remineralising agents along with biomodification of dentinal collagen for the treatment of RCLs.

In the present study, firstly, the remineralising efficacy of MIV and CPWV on RCLs was investigated using laboratory simulated RCLs *ex vivo*. The effects of 5000 ppm FTP were explored, also in combination with MIV or CPWV. Moreover, PA was used as an adjunct to MIV, CPWV and 5000 ppm FTP and their combined effects on RCLs was examined in terms

of birefringence, elemental composition, mineral density and mechanical properties of the treated root dentine.

2. Materials and Methods

2.1. Materials

Materials used were proanthocyanidin (International Laboratory. CA, USA; containing >95% oligomeric proanthocyanidins); Clinpro™ White Varnish (CPWV; 5% NaF – 22,600 ppm F with TCP; 3 M ESPE, MN, USA); MI Varnish (MIV; 5% NaF – 22,600 ppm F with RECALDENT™ (CPP-ACP); GC Corp., Tokyo, Japan); Clinpro™ 5000 ppm FTP (3 M ESPE, MN, USA) and Duraphat™ varnish (5% NaF – 22,600 ppm F; Colgate-Palmolive, NY, USA). The demineralising solution for RCL formation contained 50 mmol/L acetic acid, 2.2 mmol/L $CaCl_2$ and 2.2 mmol/L KH_2PO_4, and the solution was adjusted to pH 5 with KOH. Treatment solutions in pH-cycling included a demineralisation solution prepared using 50 mmol/L acetic acid, 1.5 mmol/L $CaCl_2$ and 0.9 mmol/L KH_2PO_4 and adjusted to pH 5 with KOH and a remineralisation solution prepared using 1.5 mmol/L $CaCl_2$, 0.9 mmol/L KH_2PO_4, 130 mmol/L KCl and 50 mmol/L HEPES buffer and adjusted to pH 7 with KOH. Details of the materials and the application methods are listed in Table 1.

2.2. Preparation of root dentine specimens

Extracted human permanent molars from individuals aged 20 to 50 were stored in 0.1% thymol solution at 4 °C under the protocol approved by the Human Research Ethics Committee of the University of Melbourne. The teeth were cleaned with deionised distilled water (DDW) to remove surface debris. Non-carious molars without obvious defects on the root surface were selected. The crown and root apical portions were removed using a slow-speed diamond saw (Isomet, Buhler Ltd, IL, USA) under water irrigation. The minimum sample size was estimated based on a power of 0.8 with a confidence level of 95% following the method in our previous study [34]. Six specimens per group were prepared for cross-sectional microhardness testing, two for micro-computed tomography (micro-CT) analysis and afterwards energy-dispersive X-ray spectroscopy (EDS) analysis and three for polarised light microscopy observation. One spare sample was prepared in each group. Therefore, 12 dentine blocks in each group were prepared from the buccal or lingual surfaces of the roots adjacent to the cementoenamel junction (CEJ) and embedded in epoxy resin (KEP epoxy, Kemet International Ltd., Kent, UK). The tooth surfaces were polished using ascending grits (320, 600, 1200, 2500) of silicon carbide (SiC) papers to expose the root dentine surface and the debris was removed by ultrasonic cleaning for 5 min in DDW. A layer of acid-resistant nail varnish was applied on the polished root surfaces to expose a window of 3 × 4 mm for treatments.

2.3. Treatment procedure

2.3.1. Demineralisation

The whole treatment procedure is illustrated in Fig. 1. The protocol for demineralisation was modified from that previously reported [32,34]. Specifically, each specimen was immersed in 20 mL of the buffered acidic demineralising solution (see 2.1), which was prepared and changed every 24 h. After demineralisation for 120 h at 37 °C, another layer of acid-resistant nail varnish approximately 1 mm wide was applied onto the exposed dentine surface to isolate part of the exposed demineralised dentine as a demineralisation baseline for comparison.

2.3.2. Treatments

Root dentine specimens were assigned randomly to the 11 treatment groups (n = 12 per group) (Fig. 2). Specifically, the DDW group served as the negative control and Duraphat™ varnish as the positive control. The 6.5% w/v PA solution was prepared by adding PA powder into DDW and mixing thoroughly by pipetting up and down to ensure uniformity. The PA solution was applied to root dentine surfaces using a micro-brush and agitating for 1 min. The excess solution was removed gently with a cotton pellet. This was followed by a further application and agitation of fresh PA solution for 1 min. MIV or CPWV was applied according to the manufacturer's instructions (Table 1).

2.3.3. pH-cycling

After treatment, all specimens were stored in a remineralisation solution (20 mL per sample) for 6 h without interference of the treated surface and then subjected to the pH-cycling process. Specifically, specimens were immersed in the demineralisation solution (see 2.1) for 1 h and remineralisation solution (see 2.1) for 23 h at 37 °C. Solutions were refreshed with each pH-cycle and the process lasted for 8 d. After each immersion in demineralisation solution for 1 h, the samples were cleaned gently using DDW and blot dried. For samples in Groups A-B, E-G, 5000 ppm FTP was applied and brushed onto the exposed dentine surface with a micro-brush for 3 min, gently cleaned using DDW and blot dried before immersion in remineralisation solution. Samples in Group C-D, H-K were gently cleaned with DDW without brushing with FTP before immersion in the remineralisation solution. After pH-cycling, samples were cleaned ultrasonically in DDW for 5 min and stored in a labelled container with damp gauze thereby creating a humidified environment before analysis.

2.4. Analytical methods

2.4.1. Polarised light microscopy

Three samples were randomly selected from each group, re-embedded in epoxy resin to protect the demineralised surfaces and sectioned longitudinally through the centre of the lesions with a low-speed water-cooled diamond saw to obtain 300 μm thick sections. During sectioning, the exposed demineralised dentine was covered with damp gauze to protect the demineralised dentine from dehydration. Each specimen was further manually lapped to a thickness of approximately 100 μm. The sample was mounted on a glass slide with DDW and covered with a clean coverslip. The slides were visualised at original 200× magnification and the birefringence was recorded using a first order red plate between crossed polarisers with transmitted light microscopy (DM2000, Leica Microsystems GmbH, Wetzlar, Germany) coupled to a camera

Table 1 – Materials used in this study.

Material brand	Abbreviation	Manufacturer	Code (Lot#)	Therapeutic composition (w/w) [35]	Application instructions
MI Varnish™	MIV	GC Corporation, Tokyo, Japan	1611141	5% sodium fluoride (NaF; 22,600 ppm F), 1–5% CPP-ACP	1. Tooth surface cleaned and softly dried using the compressed air. 2. Stir the varnish in the unit dose container and apply a thin and uniform layer of MI varnish on tooth surface using a micro-brush.
Clinpro™ White Varnish	CPWV	3 M ESPE, MN, USA	N865382	5% NaF (22,600 ppm F), 1-5% modified TCP	1. Tooth surface cleaned and softly dried using the compressed air. 2. Carefully mix the varnish with a micro-brush; apply the varnish evenly on the tooth surface.
Duraphat™	5%NaF	Colgate®, NY, USA	70091	5% NaF (22,600 ppm F)	1. Tooth surface cleaned and softly dried using the compressed air. 2. Apply a thin layer to the dentine surface using a micro-brush.
Clinpro™ 5000 toothpaste	FTP	3 M ESPE, MN, USA	131041	1.1% NaF (5,000 ppm F)	1. Brush the dentine specimen using a micro brush with the toothpaste for 3 min. 2. Rinse the specimens with deionised distilled water.
Oligomeric proanthocyanidins (>95%)	PA	International Laboratory, CA, USA	781046	A collagen cross-linking agent containing polyphenolic compounds derived from grape seed extracts.	1. Tooth surface cleaned and softly dried using the compressed air. 2. Apply on the dentine surface using a micro-brush and agitate for 1 min (two applications).

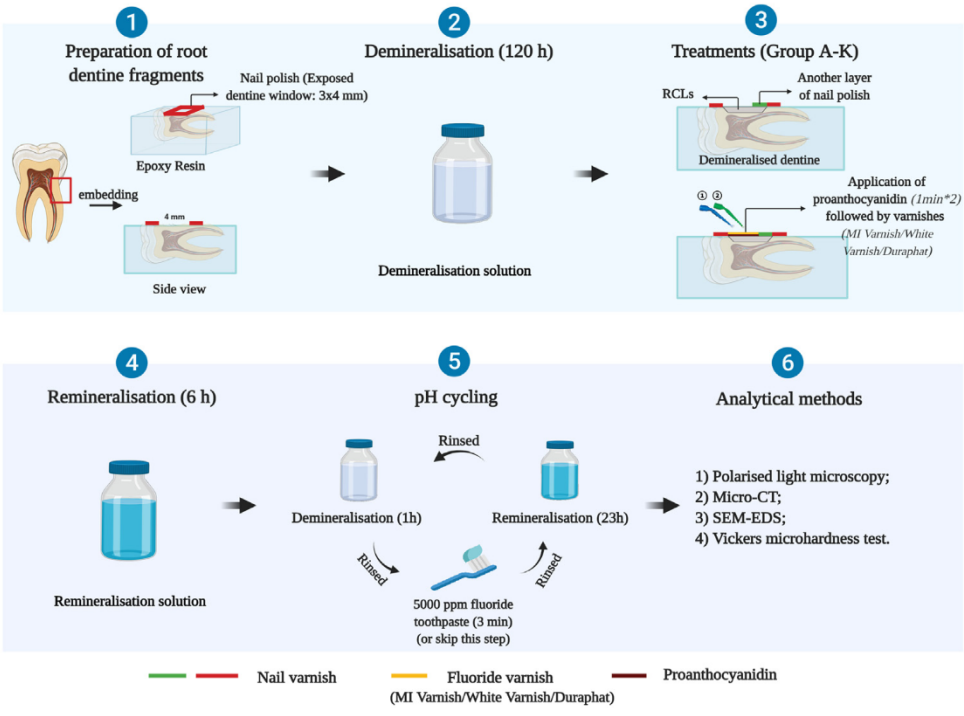

Fig. 1 – Schematic diagram of the treatment process.

(Leica EC3, Leica Microsystems GmbH, Wetzlar, Germany). The images were photographed and analysed by means of the software program Image J 1.38 × (National Institutes of Health, MD, USA).

2.4.2. *Micro-CT analysis*

Two dentine specimens randomly selected from one group were aligned in a line and fixed in a pipette tip for micro-CT scanning where a scout scan mode was used. The den-

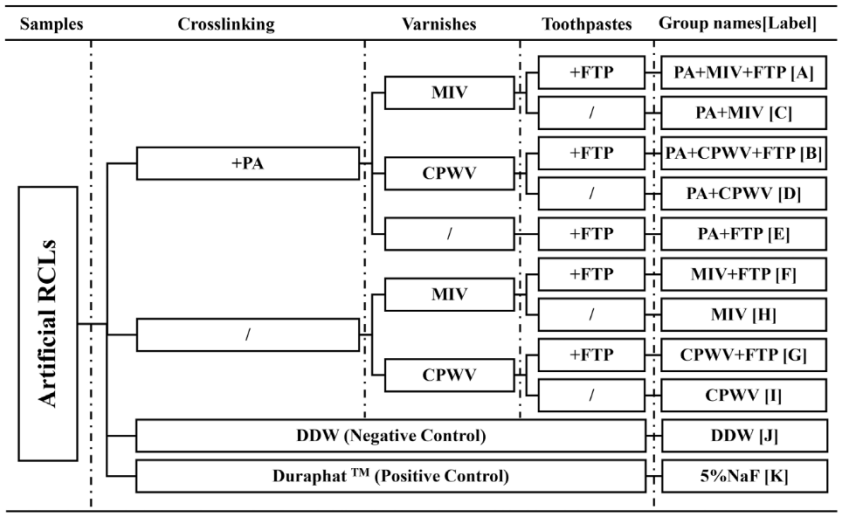

Fig. 2 – Treatments in each experimental test group and group names and labels.

tine samples were dehydrated overnight before scanning to avoid misalignment caused by shrinkage during the long-time scanning. The imaging settings for high resolution Micro-CT analysis (Skyscan 1172, Skyscan N.V., Aartselaar, Belgium) were as follows: voltage: 58 kV, beam current: 171 mA, resolution: 2.1 μm and rotation: 360° in a 0.2° step. A 0.508 mm aluminium filter was used to reduce the beam-hardening artifacts. Prior to each scanning, a new flat field reference was acquired. For calculation of mineral density, two mineral cylinder phantoms of a similar size as the specimens with the mineral density value of 0.25 and 0.75 g_{HAp}/cm^3 respectively were scanned with the same imaging settings. The resulting 2D projected images were reconstructed using the NRecon software (Version 1.4.2, Skyscan N.V., Aartselaar, Belgium) interface based on a modified Feldkamp algorithm with the following parameter settings: smoothing: 3, ring artefact correction: 15 and beam hardening correction: 50% (see Supplementary Information on beam hardening settings). After reconstruction, the reconstructed images were imported into Image J 1.38 × and resliced to obtain vertical two-dimensional slices which showed cross-sectional surfaces of whole carious lesion areas.

The mean mineral density was estimated in a volume of interest (VOI) of 30 × 20 × 250 voxels (width × thickness × depth) (30 × 2.1 × 20 × 2.1 × 250 × 2.1 μm^3) at each consecutive 2.1 μm in depth. The regions of interest (ROIs) were selected in dentine in a direction perpendicular to the lesion surface covering all lesion depths given the difficulties in selecting ROIs exactly parallel to the lesion surface in a small root dentine segment. Otherwise large heterogeneity in mineral density values of each ROI would occur. An example of a 2D image of ROI was shown in the red rectangular area in Fig. 4 (I). For each sample, three VOIs were selected randomly at the regions of demineralised dentine (covered by the second layer of nail polish), remineralised dentine (demineralised dentine exposed for treatments) and sound dentine respectively.

For the normalisation of the mineral density profile in each group, the sound dentine region covered by nail polish was used to provide a superimposition reference of the original dentine surface (depth axis of 0 μm; as shown in Fig. 4 (I)). Thus, the mineral density data were reported with the same starting point irrespective of the depths of shrinkage in the demineralised dentine regions. The mineral loss (ΔZ) across the lesion depth was calculated from the mineral density profile of each sample by subtracting the area under the mineral density curve of demineralised or remineralised dentine from the area of sound dentine. Mineral density changes predominantly occurred within the first 250 μm so the mineral loss (or gain) from the original dentine surface to a depth of 250 μm was determined.

To evaluate the extent of remineralisation, the relative mineral gain (%ΔZ) after remineralisation was calculated as follows:

$$\%\Delta Z = \frac{\Delta Zd - \Delta Zr}{\Delta Zd} \times 100$$

where ΔZd is the difference between the area under the curve (AUC) of mineral density profiles of baseline demineralised root dentine and sound dentine; ΔZr is the difference between the AUC of mineral density profiles of remineralised dentine and sound dentine; and $\Delta Zd - \Delta Zr$ is equal to the mineral gain during treatments and pH-cycling (as shown in Fig. 5A).

In order to compare %ΔZ during treatments and pH-cycling in different layers of dentine surface and subsurface, %ΔZ at 30 μm increments (a 40 μm increment for the last layer) from the dentine surface to a depth of 250 μm (*i.e.* 0-30, 30-60, 60-90, 90-120, 120-150, 150-180, 180-210 and 210-250 μm) was determined and plotted in a 3D bar graph using OriginPro 2018 (OriginLab Corporation, MA, USA).

2.4.3. *Scanning electron microscopy (SEM) and energy-dispersive X-ray spectroscopy (EDS)*

Samples used for micro-CT analysis were polished again using 2500 and 4000 SiC paper then 1 and 0.5 μm diamond suspensions in order to reduce the geometric effects on quantitative analysis by EDS; ultrasonically cleaned for 5 min to remove the polishing debris and desiccated at room temperature overnight. The cross-sectional morphology of each sample was observed by using SEM. Samples were not coated to avoid

the influence caused by the peaks of the coating material and the uncontrolled deviations due to the difference in coating thickness in quantitative EDS analysis [35]. The elemental analysis of Ca, P and F were determined using the line scan mode of EDS with a silicon drift detector (SDD) couplet to the SEM (Oxford instruments; voltage: 10.0 kV; working distance: 9.9-10.3 mm). The distance between each reading point was 1.2 μm and the live running time for each scan was 600 s to ensure sufficient counts for peak identification. Assessments of the line scan were made in triplicate in three randomly chosen areas from the lesion surface to the sound dentine along a direction perpendicular to the dentine surface in the demineralised and remineralised dentine regions. A line scan was conducted on the sound dentine area as a comparison to show the elemental changes in un-demineralised dentine. The relative X-ray intensity from EDS spectra reflecting the elemental concentrations of Ca, P and F in dentine was plotted against the lesion depth and the atomic percentage of Ca, P and F was quantified by Aztec 3.3 software (Oxford Instruments. High Wycombe, UK) available in EDS. In particular, F was included from the periodic table manually for peak identification if it was not displayed automatically due to its low concentration in the specimens.

2.4.4. *Cross-sectional microhardness test*

Six longitudinally sectioned samples in each group were re-embedded in epoxy resin and polished on a water-cooled grinding and polishing unit (Tegra-Pol 21, Struers, Copenhagen, Denmark) with abrasive papers (600, 1200, 2500 and 4000 grit), followed by 1 and 0.5 μm diamond suspensions (Type K, Kemet International Ltd., Kent, UK). The debris on the surface was removed by ultrasonically cleaning for 5 min in DDW. Cross-sectional microhardness measurements perpendicular to the demineralised surface were performed below the surface at less than 15 μm, 20 μm, 30 μm, 40 μm... to 200 μm depth with 10 μm interval using Vickers hardness indentation (402 MVD, Wolpert Wilson Instrument, MA, USA) with a load of 10 gf (98×10^{-3}N) for 10 s dwell time at each testing point. For all samples, indentations were performed on the cross-sectional dentine surface at each depth on parallel tracks approximately 150-200 μm apart both in the demineralised and remineralised dentine regions. Hardness was determined according to the following equation:

$$H = \frac{P}{A}$$

where P is the applied force and A is the contact area of the indentation which depends on the indenter geometry and the penetration depth [9]. Measurements were discarded if cracks occurred on dentine during indentation. To avoid variations of microhardness of different samples, an internal control of the sound area (250 μm depth from the surface) of each dentine block was used for comparison. Results were expressed as relative microhardness values [36].

2.5. *Statistical analysis*

Quantitative data were expressed as mean ± standard deviation (SD). The assumptions of homogeneity of variance and normal distribution were checked using Levene's and Shapiro-Wilks tests, respectively. Vickers microhardness numbers data were subject to Student's paired t-test. The relative atomic percentage (At%) data from EDS were analysed by two-way ANOVA followed by *post hoc*Bonferroni test. Other statistical analysis was carried out by one-way ANOVA and *post hoc* Tukey's (equal SD assumed) or Dunnett's T3 (equal SD not assumed) multiple comparisons. A level of significance of $\alpha = 0.05$ was set in all statistical tests (SPSS Version 22.0; IBM, NY, USA).

3. Results

3.1. *Polarised light microscopy*

Images of polarised light microscopy demonstrated the lesion depths and changes of colour birefringence which indicated the mineral content changes qualitatively during de-/remineralisation [37]. Specifically, demineralised dentine showed different birefringence from sound dentine (Fig. 3 A-K, left side of the white dotted lines). Therefore, the average lesion depth of demineralised dentine lesions (155.1 ± 23.5 μm) was determined from all the samples tested (n = 3 in each group) (Fig. 3 A; Table 2). A dark band on the dentine surface was observed in all PA-treated groups (Fig. 3 A-B & E-G). Treatment with PA + FTP produced a change of birefringence below this band in the subsurface areas of demineralised dentine, similar to sound dentine (Fig. 3 E). After treatments using either MIV or CPWV with FTP, the birefringence of demineralised dentine was reversed being similar to sound dentine (Fig. 3 C-D).

3.2. *Micro-CT analysis*

Typical 2D micro-CT images showed de-/remineralised and sound root dentine in each group (Fig. 4 (II A-K)). Shrinkage resulting from sample dehydration prior to scanning was observed in the de-/remineralised dentine regions with a grayscale value of approximately 0. Although ring artefacts corrections and flat-field corrections were applied in micro-CT reconstruction, ring artefacts can still be observed in some images (Fig. 4 (II C-E)). In addition, the influence of beam-hardening phenomenon was not eliminated, which led to the emergence of dark-streak artifacts in the reconstructed regions close to the lesion surface and might result in non-linear relationship in the conversion between X-ray attenuation and grayscale values, where the attenuation was more underestimated with increasing grayscale values [38]. Therefore, the absolute grayscale values, especially in the lesion surface areas, should be interpreted with caution.

The regression equation of the scatter plot (Fig. S2) of grayscale values versus mineral density of the two standard phantoms was used to convert the grayscales of specimens to mineral density. The mineral density profiles of specimens in each group were plotted against lesion depths (Fig. 5) and therefore the integrated mineral content throughout the lesions could be calculated according to the mineral density profiles (Table 3).

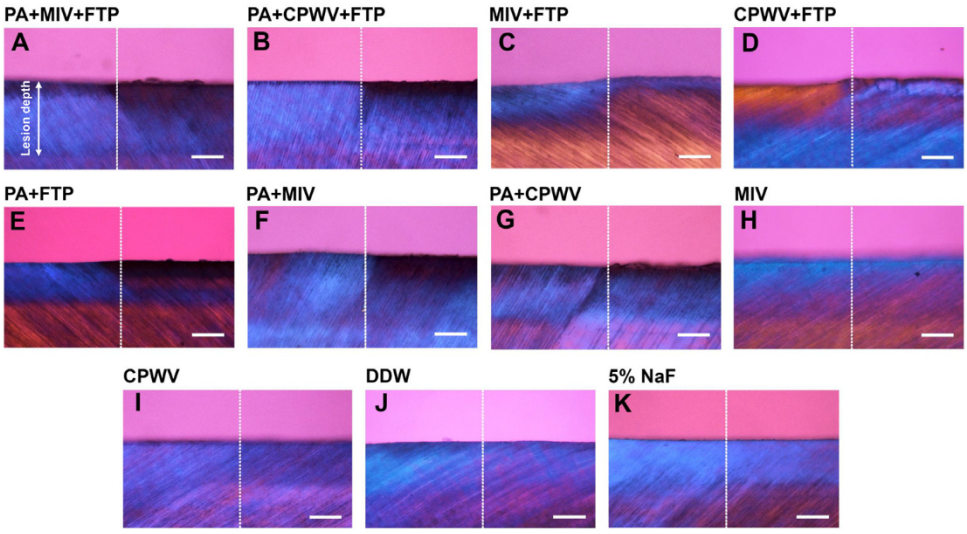

Fig. 3 – (A-K) Representative polarised light microscopy images of specimens from all the groups viewed in water (refractive index 1.33) with a first-order red plate between crossed polarisers. In each image, on the left and right side of the white dotted line is the demineralised dentine and dentine after treatments and pH-cycling respectively; Bar scale = 100 μm. The white double arrow illustrates the lesion depth.

Table 2 – Demineralised lesion depths measured under the polarised light microscopy.

Groups	Demineralised lesion depth (μm)		
	1	2	3
PA + MIV + FTP	127.2	160.4	149.3
PA + CPWV + FTP	136.6	132.5	140.3
MIV + FTP	197.2	123.9	162.1
CPWV + FTP	194.8	153.6	143.5
PA + FTP	170.8	157.8	141.3
PA + MIV	153.6	163.4	170.4
PA + CPWV	132.4	124.3	164.7
MIV	138	167	126.4
CPWV	139.6	135.6	217.8
DDW	185.2	174.6	168.2
5% NaF	127.2	160.4	149.3
Mean ± SD	155.1 ± 23.5		

Table 3 – Integrated mineral content changes of initial demineralised root dentine after each experimental phase.

Groups[a]	ΔZd	ΔZr	Mineral gain (ΔZd-ΔZr)	ΔZ% ($=\frac{\Delta Zd-\Delta Zr}{\Delta Zd} \times 100$)	Statistical analysis[b]
PA + MIV +FTP	127.39 ± 11.66	97.54 ± 7.64	29.85 ± 8.96	23.15 ± 5.56	A
MIV + FTP	124.62 ± 4.61	99.65 ± 5.98	24.96 ± 2.42	20.09 ± 2.37	A, B
PA + CPWV + FTP	152.76 ± 6.02	126.61 ± 7.33	26.15 ± 2.15	17.17 ± 1.89	B
CPWV + FTP	151.09 ± 3.24	133.73 ± 6.85	17.36 ± 4.38	11.53 ± 3.01	C
PA + MIV	177.84 ± 11.89	159.90 ± 19.03	17.94 ± 8.35	10.38 ± 5.67	C, D
PA + FTP	182.49 ± 2.71	163.87 ± 4.68	18.62 ± 3.73	10.21 ± 2.06	C, D
PA + CPWV	189.04 ± 2.84	169.98 ± 2.95	19.06 ± 1.93	10.08 ± 0.98	C, D, E
CPWV	131.20 ± 5.48	118.99 ± 5.41	12.21 ± 3.04	9.29 ± 2.24	C, D, E
MIV	142.73 ± 5.79	130.62 ± 6.94	12.12 ± 2.79	8.52 ± 2.01	D, E, F
5%NaF	154.99 ± 4.90	142.77 ± 3.55	12.22 ± 2.03	7.86 ± 1.14	E, F
DDW	131.33 ± 12.72	122.53 ± 14.66	8.80 ± 6.93	6.78 ± 5.40	F

Values are mean ± standard deviations (SD); ΔZ% is the relative mineral gain during treatments and pH-cycling.

[a] Descending order of mean ΔZ% ranks.

[b] One-way ANOVA, *post hoc* Dunnett's T3 test, $\alpha = 0.05$; different uppercase letters indicate statistically significant differences between ΔZ% values.

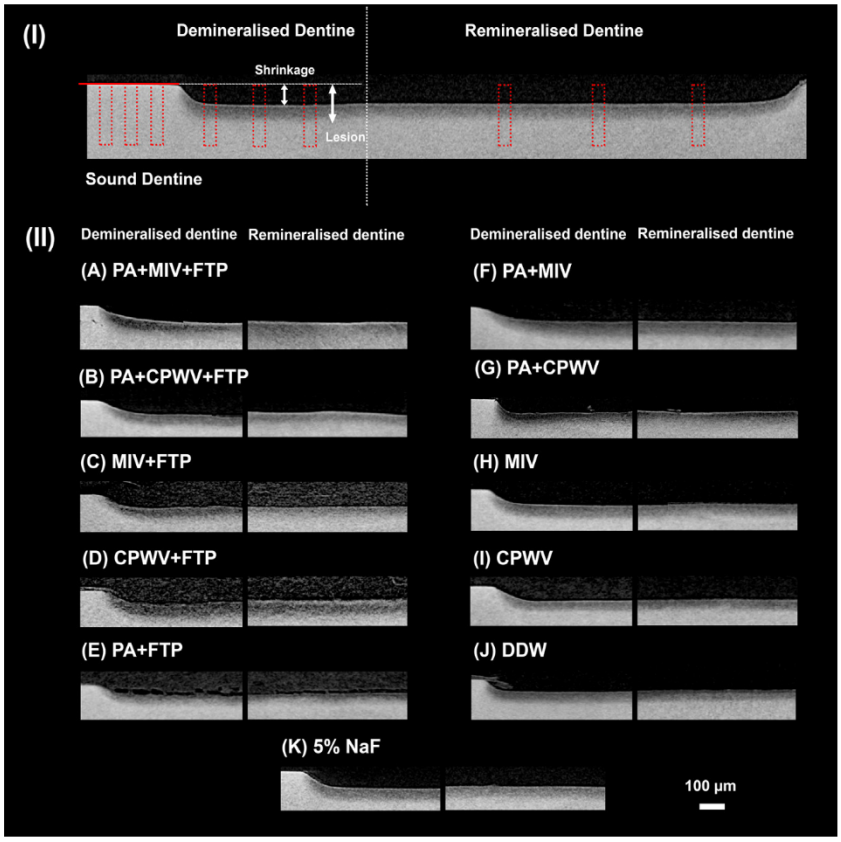

Fig. 4 – (I) An example of a two-dimensional (2D) cross-sectional slice of a specimen from micro-CT reconstruction. The red dotted boxes present the volume of interest (VOI) (30 × 2.1 × 20 × 2.1 × 250 × 2.1 μm^3 (width × thickness × depth)) over which the mineral density profiles were plotted in each specimen. Three VOIs were randomly chosen in sound, demineralised and remineralised dentine regions in each specimen. Shrinkage due to dehydration was observed in the lesion surface areas and demineralised dentine showed relatively lower grayscale values than sound dentine. (II A-K) Representative 2D micro-CT slices of sound + demineralised and remineralised dentine from all the experimental groups.

The mineral density of sound dentine (1.15 ± 0.04 g_{HAp}/cm^3) was estimated from the grayscale values of all the sound dentine tested. Demineralisation was associated with a gradual mineral loss in the dentine subsurface with relatively lower grayscale values than sound dentine (Fig. 4 (II), demineralised dentine). The convergence of the mineral density profiles of de-/re-mineralised and sound dentine regions in each group demonstrated equivalence of mineral density in the test and control sides (Fig. 5), indicating the untreated baseline demineralised dentine were a valid self-control in each group. Compared to the method of scanning the specimens after demineralisation to obtain the baseline comparison, it was more time-efficient to use the approach in the present study to obtain the mineral density values of demineralised, remineralised and sound dentine regions for comparison simultaneously and could reduce the inaccuracy from misalignment and different conditions in each scan. However, the mineral content of adjacent demineralised regions may not be exactly the same (a slight divergence of the mineral density profiles of sound dentine) because of the structural and componential anisotropy of root dentine.

Statistical analysis showed significant differences in %ΔZ after different treatments followed by pH-cycling (Table 3). Specifically, results of DDW group indicated the pH-cycling protocol used in the present study was a net-remineralising process with %ΔZ of 6.78 ± 5.40%. All the post-treatments used in the present study were associated with mineral gain throughout RCLs, but the remineralisation amount varied. Duraphat™ increased the mineral content of RCLs by 7.86 ± 1.14%, slightly higher than pH-cycling treatment alone; both MIV and CPWV further increased the mineral content of RCLs. Adjunctive application of PA with MIV, CPWV or 5000 ppm FTP showed no statistically significant difference in mineral content changes ($P > 0.05$). Generally, MIV showed greater remineralisation effects than CPWV. Specifically, combined use of MIV with 5000 ppm FTP achieved significantly higher %ΔZ compared to CPWV with 5000 ppm FTP ($P < 0.0001$). When PA was applied before the application of MIV or CPWV with FTP, the remineralisation efficacy of MIV or CPWV was significantly increased.

Relative mineral content changes post-treatment across each 30 μm increment from the original dentine surface to 250 μm depth were analysed to demonstrate the mineral con-

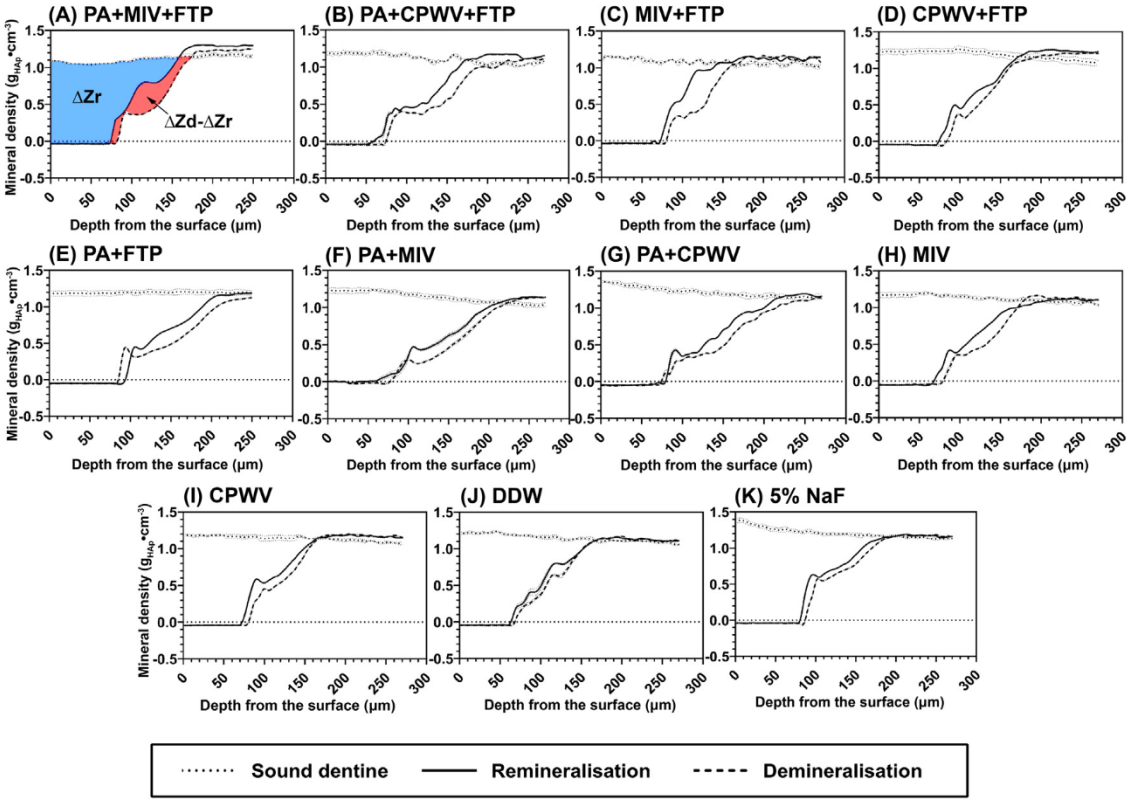

Fig. 5 – (A-K) Mineral density (g_{HAp}/cm^3) versus lesion depth profiles of VOIs in sound, demineralised and remineralised dentine regions in all the experimental groups. ΔZ was the integrated mineral loss across the lesion depth and was calculated from the mineral density profiles by subtracting the area under the curve (AUC) of demineralised or remineralised dentine from AUC of sound dentine. ΔZd−ΔZr is equal to mineral gain during treatments and pH-cycling.

tent in different surface/subsurface layers of RCLs (Fig. 6; Table S1). Shrinkage was observed at 0-60 μm depth from the original dentine surface and the mineral gain started from 60-90 μm depth in all samples. Using PA as an adjunct with F regimens (*i.e.* MIV, CPWV and FTP) led to an incremental increase of mineral density in deeper subsurface areas (especially of 150-180 μm) compared to those without PA pre-treatment.

3.3. *Scanning electron microscopy (SEM) - energy-dispersive X-ray spectroscopy (EDS)*

The EDS analysis has the advantage of detecting all elements simultaneously with high efficiency. However, compared to the high spectral resolution wavelength-dispersive spectrometer (WDS), EDS is less accurate in determining elements with low atomic number and low concentration [39]. Therefore, quantitative data obtained by EDS should be interpreted with caution. The X-ray intensity in the EDS spectra with line scan mode reflected the elemental concentration changes along the cross-sectional dentine surface from the lesion surface to the sound dentine area. The line scan conducted on the sound dentine area which served as a comparison showed a sharp decrease of elemental concentrations from dentine into the epoxy resin (Fig. S1), whilst in the demineralised dentine regions, a gradient of elemental (Ca and P) concentrations was shown from the lesion base towards the lesion surface (Fig. 7 A-K, demineralised dentine). In the remineralised dentine regions, the line scan demonstrated a slight increase of Ca, P and F concentrations throughout the artificial RCL area (Fig. 7 A-K, remineralised dentine).

From the semi-quantitative analysis (Table 4), treatment with DDW did not result in significant changes in the atomic percentage (At%) of Ca, P and F in RCLs ($P > 0.05$). The At% of Ca, P and F was increased after remineralisation in some groups compared to the demineralised dentine. Particularly, there was an increase of Ca and P in dentine surface areas when treated with PA + FTP (Fig. 7 E), although At% of Ca and P throughout RCLs was significant decreased (Table 4). Exposure to MIV or CPWV with PA and 5000 ppm FTP increased the At% of Ca, P and F significantly after pH-cycling ($P < 0.05$) and this might indicate their combined effects on ion uptake and distribution (Fig. 7 A-B; Table 4). Whilst a significant increase in At% of F throughout RCLs was observed in all experimental groups (Table 4), a less incremental increase of At% of F was present in CPWV involved groups (Fig. 7 B, D, G, I) than MIV involved groups (Fig. 7 A, C, F, H), indicating the difference in the availability of F- from varnishes incorporating Ca-P using different technologies.

3.4. *Cross-sectional Vickers microhardness testing*

The cross-sectional Vickers microhardness numbers (VHN) of dentine were slightly increased after treatments at comparative depths of demineralised dentine from less than 15 μm to

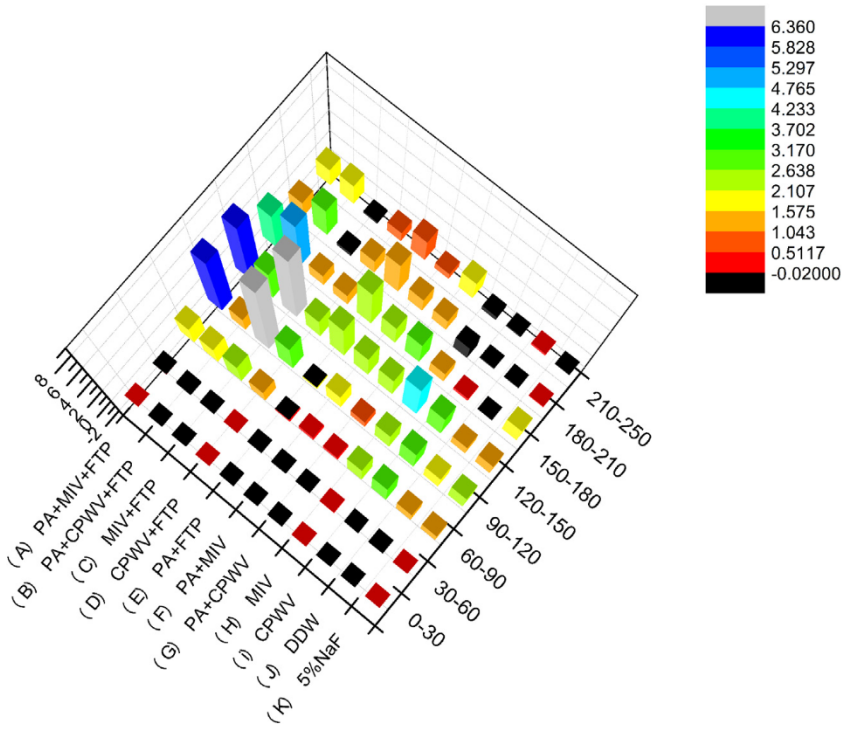

Fig. 6 – Three-dimensional (3D) bar charts of relative mineral content changes in each group after pH-cycling from ~30 μm to 250 μm depth with 30 μm increments (a 40 μm increment in the deepest layer of demineralised dentine).

Table 4 – The relative atomic percentage (At%) of calcium (Ca), phosphorus (P) and fluorine (F) in demineralised and remineralised dentine regions analysed by energy dispersive X-ray microanalysis (EDS) with a line scan mode.

Groups	Atomic percentage (At%) (Mean (SD))					
	Ca		P		F	
	Demin	Remin	Demin	Remin	Demin	Remin
PA + MIV + FTP	10.80 (0.399)	12.72 (0.160)*	7.038 (0.207)	7.911 (0.042)*	0.436 (0.002)	1.031 (0.014)*
PA + CPWV + FTP	10.47 (0.210)	12.97 (0.261)*	6.729 (0.090)	8.272 (0.090)*	0.477 (0.015)	0.675 (0.045)*
MIV + FTP	10.89 (0.038)	12.03 (0.295)*	6.866 (0.090)	7.345 (0.109)*	0.438 (0.035)	1.013 (0.082)*
CPWV + FTP	10.54 (0.178)	10.50 (0.710)	6.903 (0.054)	6.934 (0.368)	0.488 (0.039)	0.747 (0.064)*
PA + FTP	11.03 (0.203)	10.30 (0.295)*	7.130 (0.093)	6.545 (0.063)*	0.483 (0.027)	0.780 (0.017)*
PA + MIV	10.24 (0.063)	11.43 (0.182)*	6.714 (0.012)	7.583 (0.032)*	0.450 (0.031)	1.413 (0.119)*
PA + CPWV	10.38 (0.252)	9.724 (0.378)	6.470 (0.228)	6.274 (0.245)	0.407 (0.033)	0.898 (0.047)*
MIV	10.84 (0.244)	10.83 (0.316)	6.808 (0.144)	6.884 (0.232)	0.457 (0.006)	0.675 (0.014)*
CPWV	10.06 (0.190)	10.44 (0.113)	6.548 (0.235)	6.897 (0.115)*	0.513 (0.018)	0.602 (0.014)*
DDW	11.58 (0.378)	11.39 (0.569)	7.437 (0.174)	7.246 (0.333)	0.497 (0.084)	0.435 (0.046)
5%NaF	10.45 (0.158)	11.38 (0.231)*	6.653 (0.168)	7.126 (0.150)*	0.523 (0.078)	1.131 (0.073)*

The asterisks indicate statistically significant difference of At% between the demineralised and remineralised dentine in each group (two-way ANOVA, Bonferroni *post hoc* test, $\alpha = 0.05$).

100 μm in most groups although mostly without significant difference ($p > 0.05$). After treatment with Duraphat™, MIV or CPWV, the VHN of demineralised dentine did not increase significantly at all lesion depths (Fig. 8 H, I and K). Combined use of MIV with PA increased VHN of demineralised dentine up to 20 μm (Fig. 8 F) ($p < 0.05$). A significant increase in dentine surface (~15 μm depth) microhardness was observed after application of MIV (Fig. 8 C) and CPWV (Fig. 8 D) followed by pH-cycling with 5000 ppm FTP ($p < 0.05$). With adjunctive application of both PA and 5000 ppm FTP, treatment with either MIV or CPWV was associated with an increase of VHN in RCLs up to 30 μm depth ($p < 0.05$) (Fig. 8 A-B).

4. Discussion

In the present study, the remineralising effects of MIV, CPWV and high concentration (5000 ppm) FTP on artificial RCLs were investigated. PA was used as an adjunct to F regimens to putatively stabilise the demineralised dentinal collagen. The *ex vivo* artificial RCL model created by the deminer-

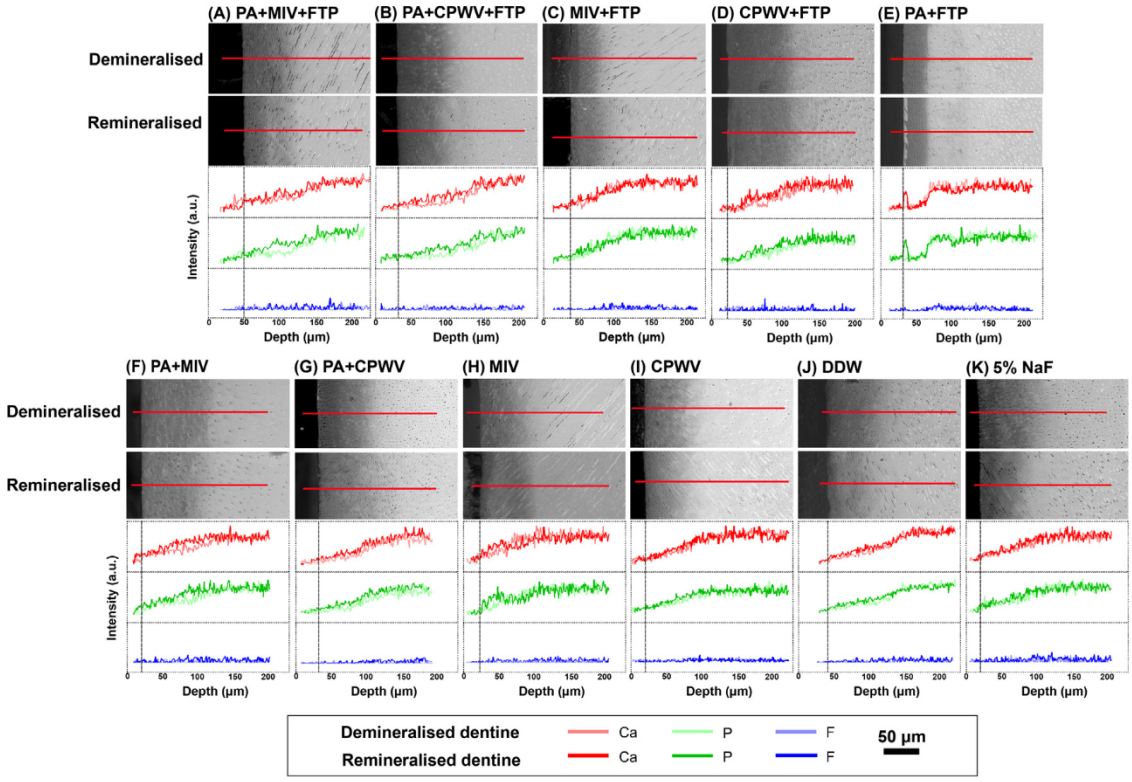

Fig. 7 – (A-K) Scanning electron microscopy (SEM) images of cross-sectional surfaces of de-/remineralised dentine and the corresponding relative concentrations of calcium (Ca), phosphorus (P) and fluorine (F) analysed by the line scan mode of SEM-energy dispersive X-ray analysis (SEM-EDS).

alising solution has high reproducibility under controlled conditions compared to natural RCLs. Nevertheless, root dentine is a material of structural anisotropy with nonidentical physicochemical characteristics in different regions and in order to minimise these variations, part of the demineralised root dentine in each specimen was kept as baseline demineralisation for comparison [40,41]. The demineralisation process led to the putative loss of dentine mineral crystals with weak negative birefringence, thus increasing the strength of positive birefringence relatively. The demineralisation solution diffused into the organic matrix and gradually dissolved the mineral components of dentine, leading to a gradient concentration decrease of Ca and P. The mineral content and microhardness were gradually reduced from the lesion surface to the sound dentine area. Specifically, micro-CT profiles in this study demonstrate a demineralised shoulder in all samples, attributed to the different rates of demineralisation of intertubular and peritubular dentine [42].

Application of varnishes and toothpastes containing F promoted the deposition of a layer with relatively high mineral density on RCL surfaces and achieved an increased concentration of F throughout RCLs. This was consistent with previous reports that F was able to incorporate minerals into dentine through partial ionic substitution for hydroxyl ions in hydroxyapatite and resulted in covalent Ca-F bonds and/or hydrogen O-H···F bonds, thus potentially forming hydroxyapatite, fluorhydroxyapatite or fluorapatite [12]. However, the unit cell volume of dentine hydroxyapatite as well as the crystalline packing and mineral-matrix interactions may have not been altered, as there were no significant changes in microhardness of dentine after treatments with FTP or Duraphat^{TM}.

MIV and CPWV used in this study utilise different techniques to keep the Ca-P based remineralisation systems in a bioavailable status and separated from F, enabling a concentration gradient for ion diffusion into demineralised dentine. Specifically, in CPP-ACP, which is contained in MIV, CPP binds to the (100) and (010) faces of apatite crystals and stabilises ionic calcium and phosphate in a metastable solution that increases the solubility of Ca-P [43]. TCP in CPWV is based on the crystalline technology which prevents the reaction between Ca^{2+} and F- by a protective fumaric acid barrier that breaks down in an aqueous environment (saliva) releasing Ca^{2+} and PO_4^{3-}. Results from the present study indicated that comparatively lower incremental increases of At% of F and mineral content were detected in RCLs treated with CPWV than MIV due to the addition of Ca-P that influences the availability of F-, as once Ca^{2+} and PO_4^{3-} were exposed to F- in an aqueous environment, they may reprecipitate quickly on the dentine surface [44]. Formation of ACP clusters by the aggregation of CPP with Ca^{2+} and PO_4^{3-} prevents their precipitation with F-, enabling a high-level release of available Ca^{2+} and PO_4^{3-}. Whilst in TCP, Ca-P was stabilised by the solid state method and might precipitate faster once exposed

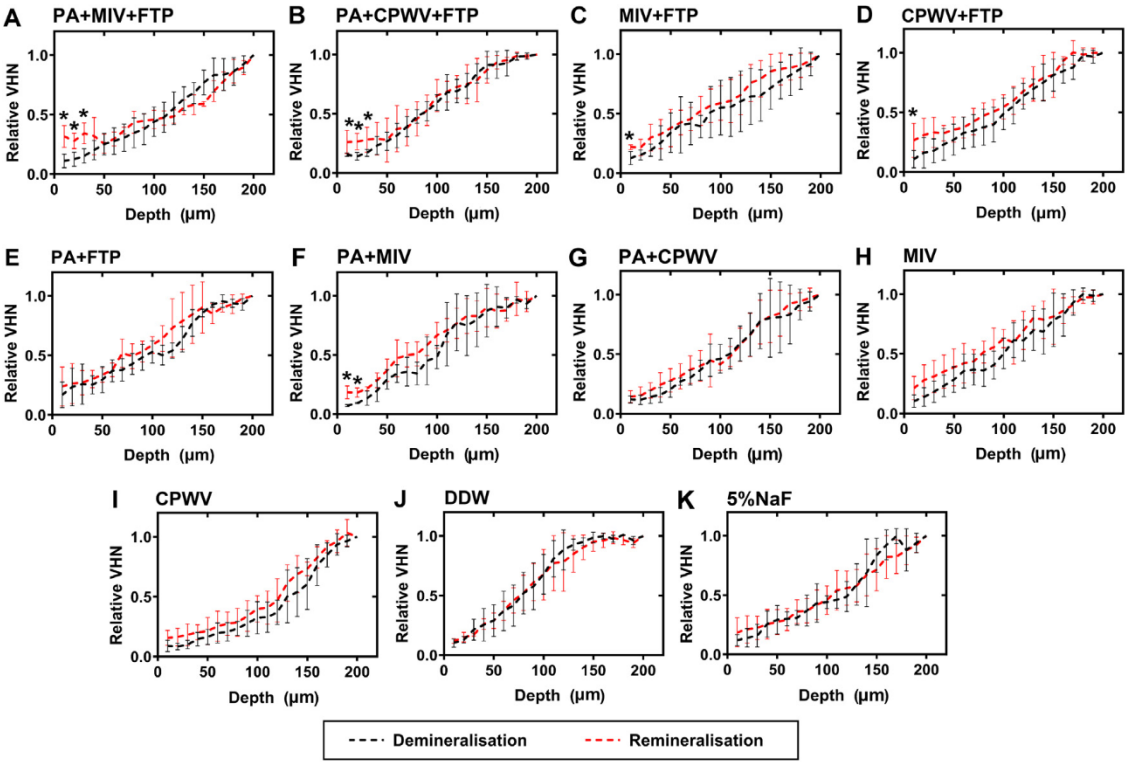

Fig. 8 – (A-K) Vickers microhardness numbers (VHN) of demineralised and remineralised dentine from less than 15 μm to 200 μm depth from the lesion surface with 10 μm interval (*i.e.* ~15 μm, 20 μm, 30 μm, 40 μm, . . . to 200 μm). Values were expressed as mean ± standard deviation (SD). The asterisks indicate statistically significant difference of VHN between the demineralised and remineralised dentine regions of a sample at the same depth (Student's t test, α = 0.05).

to the aqueous environment, depleting remineralising ions from lesion pores [45]. Moreover, CPP-ACP complexes have a higher wettability than TCP and thus have a better contact with tooth surfaces. The CPP-ACP complexes attached to dentine surfaces form a concentration gradient to maintain a state of supersaturation with respect to hydroxyapatite, therefore inhibiting the demineralisation of underlying dentine. Nevertheless, both MIV and CPWV failed to improve the microhardness of artificial RCLs. In this regard, compared to enamel, remineralisation of root dentine by MIV was more difficult to achieve in term of recovery of hardness especially in the subsurface areas due to the difficulty in achieving intrafibrillar mineralisation which determines the mechanical properties of dentine and relies upon the particular location and interaction of minerals within the dentinal organic matrix [46,47].

The benefits of combined application of F varnishes and toothpastes compared to the use of either product alone for the treatments of RCLs were also indicated. Specifically, application of MIV or CPWV along with 5000 ppm FTP reversed the birefringence of demineralised dentine being similar to sound dentine and significantly improved the surface hardness of artificial RCLs; the mineral density was further increased throughout the lesions. This was in accordance to the clinical recommendation for the use of FTP after F varnishes to maintain the presence of F, as F varnishes may not persist for long in the oral environment due to mastication, oral hygiene procedures, soft tissue movement and salivary flow [48]. It has been speculated that the high concentration F from varnishes 'pulsed' after treatment with dentifrices and this might facilitate the secondary nucleation of $Ca_5(PO_4)_3(OH)_{1-x}F_x$ or other intermediate phases of Ca-P before the formation of the more thermodynamically stable hydroxyapatite, fluorhydroxyapatite or fluorapatite phase [49].

As indicated by the micro-CT profiles, mineral gain in demineralised root dentine after treatments originated from the precipitation promoted by remineralising agents and the reprecipitation of the dissolved mineral ions from inner dentine moving outward. Particularly, the surface mineralised layer on root dentine was not prominent presumably because the outer layers of dentine had been exposed longer and affected more by acids than the inner layers. Therefore, the outer layers contained fewer residual crystals that could act as nuclei for remineralisation [50]. Also, the residual crystals may be blocked by the relatively large amount of demineralised organic matrix components, inhibiting their contact with the extrinsic remineralising ions. With less mineral loss, the inner zone at the base of the lesion was more readily remineralisable and fully recovering its properties at a rapid rate [51]. In addition, the absolute mineral density values by micro-CT analysis obtained in this study should be interpreted with caution. Specifically, samples were dehydrated before micro-CT scanning and the shrinkage caused by the dehydration could lead to an underestimation of the absolute values of total mineral loss calculated from the mineral density profiles. Nevertheless, there was a constant linear relationship between the results of mineral loss of dehydrated dentine samples accord-

ing to micro-CT profiles and the real mineral loss evaluated by chemical analysis [52]. Therefore, comparisons of the values of %ΔZ (= $\frac{\Delta Zd-\Delta Zr}{\Delta Zd}$) amongst different groups would not be influenced by dehydration.

The concept of dentine biomineralisation recognises the critical roles of the collagen matrix in orchestrating mineralisation and provides new insights into novel approaches for dentine remineralisation. In light of this, PA, an exogenous collagen cross-linker, was used in the present study to strengthen the dentinal collagen matrix, presumably promoting the formation of a mineralised matrix [27]. Application of PA tended to aggregate and cross-link the collagen fibrils and reduced interfibrillar spaces which would decrease the porosity of type I collagen, as suggested in the polarised light microscopy images by the formation of a dark band in all PA-treated dentine. Although PA alone cannot enhance intrafibrillar mineralisation, the hydroxyphenyl groups in PA may act as ligands to bind Ca^{2+} [53]. The formation of calcium-PA complexes could promote mineral deposition and attract more calcium phosphate onto the PA-modified collagen fibrils, as indicated by the increased At% of Ca and P as well as the improved %ΔZ throughout the artificial RCLs compared to treatments without PA [54]. In particular, significant %ΔZ was achieved in the subsurface areas. Results in the present study indicated the active role of collagen as a template for attracting and controlling the infiltration of Ca-P, as revealed in previous studies, *via* capillary forces, osmotic-regulated mechanisms as well as electroneutrality ($CaHPO_4$) for dentine remineralisation, following a different mechanism from the classical crystallisation of enamel [43,55].

Increased mineral content is not an appropriate endpoint of assessing the success or failure of the remineralisation effects of bioactive materials, as it was not necessarily translated into a recovery of mechanical properties. Whilst remineralisation may occur preferentially in the extra-fibrillar zone, the mineral content in the intrafibrillar compartments plays a more determinant role in the mechanical properties of dentine [56,57]. Results in the present study indicated that whilst combined use of MIV or CPWV along with 5000 ppm FTP significantly increased surface (less than 15 μm depth) microhardness, using PA as an adjunct significantly improved the subsurface microhardness up to 30 μm. It was speculated that simultaneously strengthening the dentinal matrix whilst applying the remineralising agents might prevent the partially demineralised subsurface from further mineral loss and collagen collapse as well as promote the formation of a more well-structured organic-inorganic interaction for stress redistribution during loading in microhardness testing. However, conversion of the CaF_2 -like materials deposited on lesion surfaces to fluorhydroxyapatite incorporated in dentine for the recovery of hardness is a very slow process [51]. Therefore, in the present study, after 8-day pH-cycling, microhardness of demineralised dentine only increased to a limited depth.

Of note, several aspects should be considered which may influence the remineralising efficacy of the treatments used in the current study. The pH-cycling model used included only one demineralisation phase daily, therefore the reaction products formed during pH changes and their effects on demineralisation resistance might not be pronounced. In particular, ion release from CPP-ACP could be significantly enhanced in an acidic environment [58]. Also, varnishes were not removed before pH-cycling in order to protect the remineralising surface, therefore varnishes with inferior 'adhesive properties' may detach from the dentine surface more easily, resulting in reduced effectiveness - this may also contribute partly to the large deviations of some results (*e.g.* microhardness) [44]. In addition, varnishes containing F can release F- into the surrounding medium in the oral environment and to the tooth surfaces that are not covered by varnishes. This effect of F varnishes was not evaluated in the present study. Moreover, the effects of saliva, dental plaque and enzymes and the different characteristics of natural RCLs compared to demineralised root dentine should be considered before conclusions regarding the treatment efficacy of F regimens along with collagen cross-linking agents on RCLs can be drawn.

5. Conclusion

Within the limitations of this laboratory study, in a simulated net-remineralisation oral environment, application of Duraphat™, CPWV and MIV introduced F- into artificial RCLs and slightly increased the mineral content but had no significant effects on microhardness of demineralised root dentine. When MIV or CPWV was applied in conjunction with 5000 ppm FTP, the birefringence of the demineralised dentine was reversed being similar to sound dentine and the surface (less than 15 μm) microhardness of artificial RCLs was significantly improved in addition to increased mineral content throughout the lesions. Using PA as an adjunct to F regimens improved the mineral density of demineralised root dentine significantly, especially in the subsurface areas. Pre-treating dentine with PA before application of MIV or CPWV along with 5000 ppm FTP achieved the highest ion uptake of Ca^{2+}, PO_4^{3-} and F- compared to the other treatment approaches; a significant increase of cross-sectional microhardness of demineralised dentine was observed up to 30 μm depth. Generally, MIV containing CPP-ACP was associated with a higher mineral content increase than CPWV containing TCP.

Declarations of interest

None.

Acknowledgements

This work was supported by Australian Dental Research Foundation (ADRF) Nathan Cochrane Memorial Grant and ADRF grant No. 326-2018. Jing Cai was supported by the China Scholarship Council - University of Melbourne Research Scholarship. The authors appreciate the Bio21 Advanced Microscopy Facility and Ms Su Toulson for the assistance with SEM-EDS analysis.

Appendix A. Supplementary data

Supplementary material related to this article can be found, in the online version, at doi:https://doi.org/10.1016/j.dental.2020.10.021.

REFERENCES

[1] Hariyani N, Setyowati D, Spencer AJ, Luzzi L, Do LG. Root caries incidence and increment in the population - A systematic review, meta-analysis and meta-regression of longitudinal studies. J Dent 2018;77:1–7.
[2] Selwitz RH, Ismail AI, Pitts NB. Dental caries. The Lancet 2007;369:51–9.
[3] Walls AW, Meurman JH. Approaches to caries prevention and therapy in the elderly. Adv Dent Res 2012;24:36–40.
[4] He G, Dahl T, Veis A, George A. Nucleation of apatite crystals in vitro by self-assembled dentin matrix protein 1. Nat Mater 2003;2:552–8.
[5] Veis A. Materials science. A window on biomineralization. Science 2005;307:1419–20.
[6] Bertassoni LE, Orgel JP, Antipova O, Swain MV. The dentin organic matrix - limitations of restorative dentistry hidden on the nanometer scale. Acta Biomater 2012;8:2419–33.
[7] Bertassoni LE, Habelitz S, Kinney JH, Marshall SJ, Marshall Jr GW. Biomechanical perspective on the remineralization of dentin. Caries Res 2009;43:70–7.
[8] Kuboki Y, Ohgushi K, Fusayama T. Collagen biochemistry of the two layers of carious dentin. J Dent Res 1977;56:1233–7.
[9] Pugach MK, Strother J, Darling CL, Fried D, Gansky SA, Marshall SJ, et al. Dentin caries zones: mineral, structure, and properties. J Dent Res 2009;88:71–6.
[10] Amaechi BT. Remineralisation - the buzzword for early MI caries management. Br Dent J 2017;223:173–82.
[11] Lynch RJ, Smith SR. Remineralization agents - new and effective or just marketing hype? Adv Dent Res 2012;24:63–7.
[12] Aoba T. The effect of fluoride on apatite structure and growth. Crit Rev Oral Biol Med 1997;8:136–53.
[13] Wierichs RJ, Meyer-Lueckel H. Systematic review on noninvasive treatment of root caries lesions. J Dent Res 2015;94:261–71.
[14] Narhi TO, Kurki N, Ainamo A. Saliva, salivary micro-organisms, and oral health in the home-dwelling old elderly–a five-year longitudinal study. J Dent Res 1999;78:1640–6.
[15] Shen P, Bagheri R, Walker GD, Yuan Y, Stanton DP, Reynolds C, et al. Effect of calcium phosphate addition to fluoride containing dental varnishes on enamel demineralization. Aust Dent J 2016;61:357–65.
[16] Karlinsey RL, Mackey AC, Walker ER, Frederick KE. Preparation, characterization and in vitro efficacy of an acid-modified beta-TCP material for dental hard-tissue remineralization. Acta Biomater 2010;6:969–78.
[17] Wierichs RJ, Stausberg S, Lausch J, Meyer-Lueckel H, Esteves-Oliveira M. Caries-Preventive Effect of NaF, NaF plus TCP, NaF plus CPP-ACP, and SDF Varnishes on Sound Dentin and Artificial Dentin Caries in vitro. Caries Res 2018;52:199–211.
[18] Sleibi A, Tappuni AR, Davis GR, Anderson P, Baysan A. Comparison of efficacy of dental varnish containing fluoride either with CPP-ACP or bioglass on root caries: Ex vivo study. J Dent 2018;73:91–6.
[19] Tay FR, Pashley DH. Guided tissue remineralisation of partially demineralised human dentine. Biomaterials 2008;29:1127–37.
[20] Jiao K, Niu LN, Ma CF, Huang XQ, Pei DD, Luo T, et al. Complementarity and Uncertainty in Intrafibrillar Mineralization of Collagen. Adv Funct Mater 2016;26:6858–75.
[21] Liu Y, Kim YK, Dai L, Li N, Khan SO, Pashley DH, et al. Hierarchical and non-hierarchical mineralisation of collagen. Biomaterials 2011;32:1291–300.
[22] Bedran-Russo AK, Pauli GF, Chen SN, McAlpine J, Castellan CS, Phansalkar RS, et al. Dentin biomodification: strategies, renewable resources and clinical applications. Dent Mater 2014;30:62–76.
[23] Tjaderhane L, Buzalaf MA, Carrilho M, Chaussain C. Matrix metalloproteinases and other matrix proteinases in relation to cariology: the era of' dentin degradomics'. Caries Res 2015;49:193–208.
[24] Garcia MB, Carrilho MR, Nor JE, Anauate-Netto C, Anido-Anido A, Amore R, et al. Chlorhexidine Inhibits the Proteolytic Activity of Root and Coronal Carious Dentin in vitro. Caries Res 2009;43:92–6.
[25] Osorio R, Yamauti M, Osorio E, Ruiz-Requena ME, Pashley DH, Tay FR, et al. Zinc reduces collagen degradation in demineralized human dentin explants. J Dent 2011;39:148–53.
[26] Deyhle H, Bunk O, Muller B. Nanostructure of healthy and caries-affected human teeth. Nanomedicine 2011;7:694–701.
[27] Gu L, Shan T, Ma YX, Tay FR, Niu L. Novel Biomedical Applications of Crosslinked Collagen. Trends Biotechnol 2019;37:464–91.
[28] Bedran-Russo AK, Castellan CS, Shinohara MS, Hassan L, Antunes A. Characterization of biomodified dentin matrices for potential preventive and reparative therapies. Acta Biomater 2011;7:1735–41.
[29] Bedran-Russo AK, Karol S, Pashley DH, Viana G. Site specific properties of carious dentin matrices biomodified with collagen cross-linkers. Am J Dent 2013;26:244–8.
[30] Shavandi A, Bekhit AEA, Saeedi P, Izadifar Z, Bekhit AEA, Khademhosseini A. Polyphenol uses in biomaterials engineering. Biomaterials 2018;167:91–106.
[31] Xie Q, Bedran-Russo AK, Wu CD. In vitro remineralization effects of grape seed extract on artificial root caries. J Dent 2008;36:900–6.
[32] Epasinghe DJ, Kwan S, Chu D, Lei MM, Burrow MF, Yiu CKY. Synergistic effects of proanthocyanidin, tri-calcium phosphate and fluoride on artificial root caries and dentine collagen. Mater Sci Eng C Mater Biol Appl 2017;73:293–9.
[33] Epasinghe DJ, Yiu C, Burrow MF. Synergistic effect of proanthocyanidin and CPP-ACFP on remineralization of artificial root caries. Aust Dent J 2015;60:463–70.
[34] Cai J, Burrow MF, Manton DJ, Tsuda Y, Sobh EG, Palamara JEA. Effects of silver diamine fluoride/potassium iodide on artificial root caries lesions with adjunctive application of proanthocyanidin. Acta Biomater 2019;88:491–502.
[35] Newbury DE, Ritchie NW. Is scanning electron microscopy/energy dispersive X-ray spectrometry (SEM/EDS) quantitative? Scanning 2013;35:141–68.
[36] Chu CH, Mei LEI, Seneviratne CJ, Lo ECM. Effects of silver diamine fluoride on dentine carious lesions induced by Streptococcus mutans and Actinomyces naeslundii biofilms. Int J Paediatr Dent 2012;22:2–10.
[37] Theuns HM, Shellis RP, Groeneveld A, van Dijk JWE, Poole DFG. Relationships between Birefringence and Mineral Content in Artificial Caries Lesions of Enamel. Caries Res 1993;27:9–14.
[38] Zou W, Hunter N, Swain MV. Application of polychromatic microCT for mineral density determination. J Dent Res 2011;90:18–30.
[39] Newbury DE, Ritchie NW. Quantitative Electron-Excited X-Ray Microanalysis of Borides, Carbides, Nitrides, Oxides,

and Fluorides with Scanning Electron Microscopy/Silicon Drift Detector Energy-Dispersive Spectrometry (SEM/SDD-EDS) and NIST DTSA-II. Microsc Microanal 2015;21:1327–40.
[40] Wang R, Weiner S. Human Root Dentin: Structural Anisotropy and Vickers Microhardness Isotropy. Connect Tissue Res 2009;39:269–79.
[41] Forien J-B, Zizak I, Fleck C, Petersen A, Fratzl P, Zolotoyabko E, et al. Water-Mediated Collagen and Mineral Nanoparticle Interactions Guide Functional Deformation of Human Tooth Dentin. Chem Mater 2016;28:3416–27.
[42] Kinney JH, Balooch M, Haupt Jr DL, Marshall SJ, Marshall Jr GW. Mineral distribution and dimensional changes in human dentin during demineralization. J Dent Res 1995;74:1179–84.
[43] Cochrane NJ, Cai F, Huq NL, Burrow MF, Reynolds EC. New approaches to enhanced remineralization of tooth enamel. J Dent Res 2010;89:1187–97.
[44] Cochrane NJ, Shen P, Yuan Y, Reynolds EC. Ion release from calcium and fluoride containing dental varnishes. Aust Dent J 2014;59:100–5.
[45] ten Cate JM. Remineralization of Caries Lesions Extending into Dentin. J Dent Res 2001;80:1407–11.
[46] Bertassoni LE, Habelitz S, Marshall SJ, Marshall GW. Mechanical recovery of dentin following remineralization in vitro–an indentation study. J Biomech 2011;44:176–81.
[47] Bakry AS, Abbassy MA. Increasing the efficiency of CPP-ACP to remineralize enamel white spot lesions. J Dent 2018;76:52–7.
[48] Petersson LG. The role of fluoride in the preventive management of dentin hypersensitivity and root caries. Clin Oral Investig 2013;17(Suppl 1):S63–71.
[49] Nancollas GH. The mechanism of biological mineralization. J Cryst Growth 1977;42:185–93.
[50] Preston KP, Smith PW, Higham SM. The influence of varying fluoride concentrations on in vitro remineralisation of artificial dentinal lesions with differing lesion morphologies. Arch Oral Biol 2008;53:20–6.
[51] Burwell AK, Thula-Mata T, Gower LB, Habelitz S, Kurylo M, Ho SP, et al. Functional remineralization of dentin lesions using polymer-induced liquid-precursor process. PLoS One 2012;7:e38852.
[52] Ten Cate JM, Nyvad B, Van de Plassche-Simons YM, Fejerskov O. A quantitative analysis of mineral loss and shrinkage of in vitro demineralized human root surfaces. J Dent Res 1991;70:1371–4.
[53] Epasinghe DJ, Burrow MF, Yiu CKY. Effect of proanthocyanidin on ultrastructure and mineralization of dentine collagen. Arch Oral Biol 2017;84:29–36.
[54] Tang CF, Fang M, Liu RR, Dou Q, Chai ZG, Xiao YH, et al. The role of grape seed extract in the remineralization of demineralized dentine: micromorphological and physical analyses. Arch Oral Biol 2013;58:1769–76.
[55] Niu L-N, Jee SE, Jiao K, Tonggu L, Li M, Wang L, et al. Collagen intrafibrillar mineralization as a result of the balance between osmotic equilibrium and electroneutrality. Nat Mater 2016;16:370.
[56] Schwendicke F, Eggers K, Meyer-Lueckel H, Dorfer C, Kovalev A, Gorb S, et al. In vitro Induction of residual caries lesions in dentin: comparative mineral loss and nano-hardness analysis. Caries Res 2015;49:259–65.
[57] Bertassoni LE. Dentin on the nanoscale: Hierarchical organization, mechanical behavior and bioinspired engineering. Dent Mater 2017;33:637–49.
[58] Zalizniak I, Palamara JE, Wong RH, Cochrane NJ, Burrow MF, Reynolds EC. Ion release and physical properties of CPP-ACP modified GIC in acid solutions. J Dent 2013;41:449–54.